Analysis of the Pantograph-Catenary Interface Quality for the National Overhead Contact Lines and Train Pantographs

Ana Matilde Esteves Macedo

a.matilde.e.macedo@tecnico.ulisboa.pt

Instituto Superior Técnico, Universidade de Lisboa, Portugal

December 2021

Abstract

The railway systems play a pivotal role in the transport of passengers and goods, not only because of its cost, safety and comfort. But also because of its smaller carbon footprint. Increasing the competitiveness of rail transport requires that not only its operating speeds increase, but also that it is more energy efficient. The interface between the pantograph and the catenary affects the quality of the transmission of electrical energy from the infrastructure to the vehicle's electric motors, being currently the greatest technological obstacle to increasing the speed of operation of trains on the railway lines. This work aims to study two distinct catenaries in order to assess the limits to the operating speed of railway vehicles and the criteria that prevent higher speeds. This study will also focus on how distinct pantographs can affect the pantograph-catenary interaction. For this, a series of tests will be developed in order to understand the dynamics of each catenary pantograph pair, for when the catenaries are subject to operations with single or multiple pantographs. Consequently, it will be known which is the best pantograph to use with each catenary, as well as the possible loss of operating speed of the catenaries, if the pantograph with the lowest contact capacity is chosen

Keywords

Railway dynamics; Pantograph-Catenary interaction; Multiple pantograph operation; Contact force.

1. Introduction

The railway system is an important network which allows the safe transportation of goods and passengers across different points in the world. In these systems, the transference of energy occurs from the catenaries to the pantographs, therefore the contact pantograph-catenary is an important factor to take into consideration. The catenary is an overhead structure, whose purpose is to carry electric energy. The pantograph is a device mounted on top of the railway vehicle. Whose objective is to carry the energy from the catenary contact wire to the railway vehicle motor. The limiting factor of the maximum velocity achieved by the railway vehicle is the ability to maintain this contact as uninterrupted and as constant as possible [1]. This occurs because the railway vehicle motors need to receive the necessary electrical energy for their proper operation. Increasing the mean contact force would imply a better contact between the catenary and pantograph. However, it increases the component wear, due to the involved friction in the contact [2,3]. So a balance between the characteristics of the contact and the system wear generated is of utmost importance. The parameters required to evaluate the contact according with the norm EN50367 are the mean contact force, the standard deviation, the maximum contact force, the maximum steady arm uplift, and the contact loss percentage.

In order to obtain higher operating speeds for catenaries, initially designed for lower velocities requirements some changes in the catenary structures are needed. One way to obtain higher speeds is by increasing the tension on the wires by lowering the contact wire linear mass. Both of these changes lead to a higher elastic wave propagation speed, which in turn results in better contact quality. For both stitch and simple catenary types there is a pre-sag of 1/1000 to further improve the uniformity of the stiffness [4–6]. Different pantograph-catenary pairs may show significant differences in their dynamic analysis. So, it is necessary to study the required pantograph-catenary interaction for all of the pantographs that are expected to operate in that catenary. For this, the computational code *PantoCat* [7] which allows for the dynamic analysis of catenary finite element models and pantograph multibody models is extensively used in this work.

This study as an objective to analyse the dynamic behaviour of two different catenaries, in order to identify their trains speeds at which they can be operated. In order to further study their operation range, cases with single and multiple pantographs are considered. The contact quality is studied for five different scenarios for each catenary. These studies consider the overlapping zone of the catenary, i.e., the transition between two catenary sections, that represents a singularity in the catenary. Using the *PantoCat* software the dynamic results for the catenary pantograph interaction are obtained to be analysed.

2. Pantograph-Catenary Dynamics and Numerical Modelling

Railway catenaries are periodic structures mounted along the railway track. A typical construction presented in Figure 2.1 (a) includes the support, console, and stay, that supports the messenger wire and the contact wire [8]. The steady arm ensures not only the necessary stagger of the messenger and contact wire, but also the correct compliance with the supports. Finally, there are the droppers which help the connect the contact wire to the messenger wire, supporting and the contact wire and controlling the contact wire elasticity and sag i.e., the contact wire geometry. Occasionally one can also find a stitch wire in the connectivity of the messenger wire with the stay to improve the uniform stiffness around the steady arm.

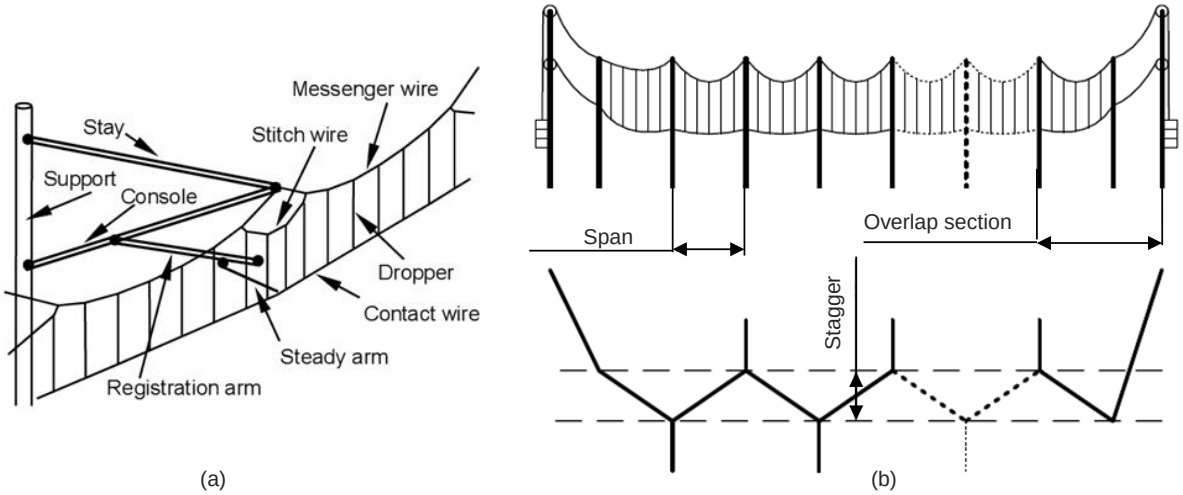

Figure 2.1: (a)Structural elements of a typical catenary (b) Side and top views of a catenary section

The contact wire and the messenger wire are tensioned, with high axial forces, to ensure sag and uniform stiffness. Each catenary section has a maximum length of 1.5 km, for geometric and costs reasons. So, each track requires several catenary sections in succession. The continuity of the contact between the pantograph and the catenary is essential, this problem is fixed by the overlapping section at the start and end of each section, represented in Figure 2.1 (b), i.e., sections composed by a span that overlaps the existing and incoming contact wires of two sequential sections and spans that connect the catenary section to the “hanging masses” [8]. The stagger is the lateral displacement of the contact and messenger wire, shown in Figure 2.1 (b). Its purposes is to ensure that the pantograph registration strip suffers an even wear along its length.

There are two main issues in the modelling of the catenary, these are the line tension and the dropper slacking. The line tension is normally achieved by a weight pulley system mounted at each end of the catenary section. This mechanism ensures the line tension of the catenary wires is kept as constant as possible to maintain the correct geometry and the limit the contact wire sag. However, the existence of pre-sag can be important to ensure a more constant contact wire stiffness [4–6]. The wave propagation speed of the contact wire is called critical velocity and it is higher than the train speed to ensure that the system is stable enough to guarantee the contact quality [9].

The dropper slacking, i.e. the dropper bending due to its compression instability represented in has a nonlinear behaviour. The dropper's purpose is to support the contact wire, maintaining it in the correct position. Therefore, droppers have a constant stress tension until the pantograph passes under them. At this point in time the dropper

loses the tension force and is suddenly subjected to compression forces. However, droppers are cables, so they offer no resistance against compression forces, which constitutes a nonlinearity that requires that the numerical methods used in the analysis can handle them. Since these nonlinearities are localized and have a known behaviour. They can be solved using corrective measure [6].

When modelling the catenary only its deformed geometry is known, i.e., the geometry that results from the application of the gravitational force and the tension forces on an unknown initial geometry. However, the geometry that can be modelled is the unknown undeformed geometry, which creates a serious initialization modelling problem. Which consists in finding the undeformed catenary geometry, that, after loading, leads to the deformed geometry already known. This requires an inverse initial problem to be solved, known as catenary model initialization. Figure 2.2 represents the side and sag view of the same catenary finite element model after the natural loads are applied.

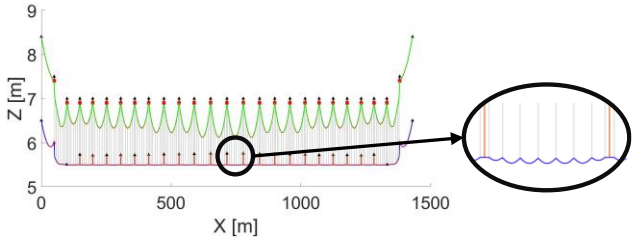

Figure 2.2: Side and sag view of a generic loaded catenary model

The catenary initialization is a minimalization problem where the objective function finds the length of each dropper so that the difference between the statistical deformed catenary geometry and the undeformed geometry is minimized. This problem is described as:

$$min\left(\sum_{1}^{m}\left\|\boldsymbol{d}_{CW}^{m}(x)-\boldsymbol{d}_{CW}^{S}\right\|\right) \qquad (2.1)$$
$$subject\ to\ x\colon [\boldsymbol{l}_0^1, \boldsymbol{l}_0^2, \dots, \boldsymbol{l}_0^m]$$

Where the initial length of each dropper i, a design variable known for each catenary model, is represented as $\boldsymbol{l}_0^i$. The nominal contact wire position at each dropper is set as $\boldsymbol{d}_{CW}$, while the already deformed contact wire position is represented as $\boldsymbol{d}_{CW}^S$. The minimization problem is solved, firstly for each span. Afterwards, the iteration process on the entire optimization problem is repeated, until convergence is obtained. It is common that three turns are enough when starting with initial dropper lengths close to those of the deployed catenaries. The farther away the initial length of the dropper is to the deployed the worst the catenary model is and the less accurate the results obtained from further studies of this catenary are if extra iterations are not used in this tunning.

When a railway vehicle passes in a track, it disturbs the catenary creating a motion that is defined by small deformations and rotations of the complete system which is nonlinear. The single source for the nonlinear response is the dropper slacking. This makes the linear finite element method ideal for the catenary system modelling and analysis, provided that the nonlinear dropper slacking can be handled efficiently. [10,11]

The computational code PantoCat, used in this work, includes a Newmark time integration algorithm [10,12] with a trapezoidal rule to solve the governing dynamic equilibrium equations. This particular method is applied due to its unconditional stability nature when used implicitly and its proven robustness in FEM applications of the type of the ones used in this work [6].

The pantograph collects the energy from the catenaries and transfers it to the train motors. A good model of the pantograph is essential to be able to obtain reliable results for the dynamic interaction with the catenary. The pantographs are generally modelled as linear lump-mass models. Even though nonlinear multibody models can be used, the lump-mass model is more commonly applied due to its simplicity. The parameters of the lump-mass

models cannot be measured experimentally or modelled by any process; therefore, they have no physical meaning. The characteristics of these models are obtained by knowing the frequency and amplitude of the motion of the pantograph when excited in a specialized test rig and by matching the lump-mass model response that was acquired experimentally [1,13].

To find the exploration velocity that a railway vehicle can travel, it is necessary to know the catenary and the pantograph that are in operation. Different catenary pantograph pairs leads to different operating conditions and, consequently, are subjected to different velocities of exploration. In order to identify the exploration velocity in a particular catenary several quantities associated to the contact force must be measured and verified.

The contact between the catenary and the pantograph is enforced by an uplift force f_{up}, pantograph. This force is constant throughout the operation and needs to be calculated, in such a way that the mean contact force, F_m, between the pantograph and the catenary follows the standards EN50367. The standard EN50367 specifies that the F_m must be inside the interval defined by two predefined values designated by minimum mean contact force $F_{m,min}$ and the maximum mean contact force $F_{m,max}$, for analysis of the quality of the contact. The contact quality is evaluated by a series of statistical measures of the contact force, F_c, resulting from the interaction pantograph-catenary. The norms also stipulate a series of parameters that the F_c and their statistical measures must verify for an acceptable operation velocity. These limit parameters can be observed in Table 2.1. When one of these parameters, exceeds the threshold, the railway vehicle is prevented to operate at that speed.

Table 2.1: Contact quality validation parameters according to EN50367

	v ≤ 200 km/h	200 km/h < v ≤ 250 km/h	v > 250 km/h
$F_{m,min}$ [N]	$0.00047v^2+60$		
$F_{m,max}$ [N]	$0.00047v^2+90$	$0.00097v^2+70$	
$F_{c,max}$ [N]	300	350	
σ_{max} [N]	≤ 0.3 F_m		
Statistical minimum [N]	> 0		
Steady arm uplift [mm]	≤ 120		
Contact loss [%]	≤ 0.1		≤ 0.2

The parameters stipulated by the norms and presented in Table 2.1 are the mean contact force F_m, maximum contact force F_{max}, as well as the statistical measures of the contact force defined by the standard deviation, σ, the statistical minimum, S_{min}, and the contact loss percentage $CL_{\%}$. A negative value of S_{min} implies a possibility of contact loss. These statistical values are obtained by the assumption in a realistic situation the contact force behaves like a normal distribution [14].

3. Subsystem modelling

The objective of this work consists of evaluating the limits of the operation condition of two different catenaries operating with two types of generic pantographs that equip the railway vehicle in exploration. In this study, both catenaries are modelled with multiple sections and, therefore, with overlapping sections, on a straight track scenario. The simulation considers the pairing of each pantograph with each of the catenaries. The LP10 catenary is simulated with a single and multiple pantograph operations for a broad range of vehicle velocities. While the LP12 catenary is only operated with a single pantograph. For the multiple pantograph operations considered each simulation scenario involves a different pantograph separation. The distance between these two pantographs corresponds to common pantograph locations in the train operations with multiple units.

3.1. Pantograph Models

Two generic pantographs are modelled in this work and designated Pant1 pantograph and Pant2 pantograph. These pantographs are modelled via lump-mass models. The car height for both pantographs is assumed to be 4 m i.e., it is assumed that they are mounted on the roof of the railway vehicle.

Table 3.1 represents the Pant1 pantograph lump-mass being its modelling parameters shown also. This table shows that the Pant2 pantograph model has an unusual topology. Since contrary to the previous, it includes four masse, nonlinear springs, and a bump-stop between m_3 and m_4.

Table 3.1 Pant1 pantograph lump-mass model and parameters

Parameter	M_1	M_2	M_3	M_4	C_1	C_2	C_3	C_4	K_1	K_2	K_3	K_4
Unit	KG	KG	KG	KG	Ns/m	Ns/m	Ns/m	Ns/m	N/m	N/m	N/m	N/m
WBL	10.15	10.45	2.88	2.88	60	0	0	0	80	13500	k(s)	k(s)
CX	4.5	6.27	4.27	-	54.1	0	30	-	1	8000	7000	-

The Pant2 pantograph lump-mass model has two equal nonlinear springs, each of them is supporting one mass. The variation of the spring length is given as

$$s_i = \left| L_i^0 - L_i \right| \tag{3.1}$$

Where L_i^0 represents the undeformed length of the spring and L_i represents the length of the spring in the current time step. This pantograph model has a bump-stop spring that limits the compression of K_3 and K_4. In this model, the bump-stop is represented using a spring with a large rigidity that starts acting when the s_i value surpasses 52 mm. The nonlinear upper mass suspension spring stiffness is given as

$$k_i(s) = \begin{cases} 2200, & if \quad 0 \le s_i < 10\ mm \\ 2500, & if\ 10 \le s_i < 20\ mm \\ 3050, & if\ 20 \le s_i < 30\ mm \\ 3650, & if\ 30 \le s_i < 40\ mm \\ 4600, & if\ 40 \le s_i < 52\ mm \\ 10^6, & if\ s_i \ge 52\ \ mm \end{cases} \tag{3.2}$$

3.2. Catenary Models

The catenaries modelled are designated by LP10 and LP12. These catenaries include various sections, each one with maximum length of 1431 m. The catenary sections include four different types of spans. Table 3.2 presents the parameters requires for the modelling for both catenaries. Where the main differences between them is the tension in the wires, T_c, and the pre-sag. The T_c is 10 km and 12 kN for LP10 and LP12 respectively, while the pre-sag is 0‰ and 1‰ respectively.

Table 3.2: Catenaries modelling parameters

Catenary length [m]		1431	Contact wire height [m]	5.5
Number of spans		26	Nº Droppers/Span	8 - 9
Nº Spans at nominal height [m]		26	Inter-dropper distance [m]	2.25-9
Span length [m]*		49.5 - 63	Stagger [m]	+/- 0.200
	Contact wire	Messenger wire	Droppers	Steady arm
Section [m^2]	1.07×10^{-4}	6.50×10^{-5}	1.20×10^{-5}	2.16×10^{-4}
Linear Mass [kg/m]	0.951	0.59	0.11	0.489
Young Modulos [Pa]	1.2×10^{11}	8.5×10^{10}	8.500×10^{10}	7.0×10^{10}
Tension [N]	T_c	T_c	-	-
Claw/Clamp mass [kg]	0.175	0.175	-	0.55
Length [m]	-	-	variable	1.168
Mass [kg]	-	-	-	0.572

The catenaries have a different initial sag value, being LP10 the catenary where the initial sag is 0‰, and LP12 the catenary where the initial sag is 1‰. The size of the pre-sag has an impact on the initial length of the droppers to consider. Table 3.3 indicates pre-sag [mm] of each dropper according to the span length for the LP12 catenary.

Table 3.3: Pre-sag initial geometric parameters of the LP12 catenary

Span [m]	Dropper nº							
	1	2	3	4	5	6	7	8
63	0	2.572	4.958	6.151	6.151	4.958	2.572	0
58.5	0	2.559	4.388	5.688	5.688	4.388	2.559	0
54	0	2.544	4.686	5.400	4.686	2.544	0	
49.5	0	2.525	4.158	4.950	4.158	2.525	0	

4. Dynamic Analysis of Pantograph Catenary Interaction

The objective of this work is to determine the operational conditions of two different catenary models, LP10 and LP12, in interaction with two different pantographs, Pant1 and Pant2. In this sense, five different case scenarios are here considered, for each different pantograph-catenary pair. One scenario consists in the study of the pantograph-catenary interaction when there is a single operating pantograph, while the other four scenarios consider catenary operations with multiple pantographs. Moreover, at each of these case scenarios, the evaluation of the pantograph-catenary behaviour is analysed at different speeds and pantographs separations.

The zone of interest considered starts at 900m and ends at 1705m, for both catenaries One of the reasons why the zone of interest is here is the existence of the overlapping near the middle of this zone. Another reason for this choice is the ability to study the contact parameter for many span lengths.

For ease of reference, each of the full set of pantograph-catenary analyses performed in this work is identified following the designation “Cat_Pant_SXXX_VYYY”, where Cat refers the corresponding evaluated catenary model. Pant refers to the type of pantograph used. XXX is the value of the pantograph separation, in meters and YYY is the train speed, in km/h.

4.1. Single Pantograph

Looking at the LP10 catenary paired with the Pant1 pantograph the exploration velocity is found to be 170 km/h for a single pantograph train operation, which is 88 km/h lower than the maximum operating velocity of 258 km/h. The limiting parameter of this pantograph-catenary pair is the maximum contact force seen in Table 4.1that is located in the section of the catenary with the overlap. Comparing the cases with the Pant1 pantograph and the Pant2 pantograph, it is possible to observe that the limiting parameter of this pantograph-catenary pair is also the maximum force,

Table 4.2. However, the Pant2 operation has a lower exploration velocity, that is found to be 165 km/h for a single pantograph train operation, this is a little bit lower than when using the Pant1 pantograph and it is close to 93 km/h lower than the maximum operating velocity. This pantograph catenary case also has the same limiting factor, maximum contact force. By comparing the dynamic analysis results for both pantographs, it is found that the standard deviation has higher values and lower the statistical minimum for the Pant2 pantograph. So even if the maximum force threshold is not surpassed, the Pant2 pantograph has a worst contact interaction with the catenary.

Table 4.1: LP10_Pant1_S0 results for simgle pantograph, running at various speeds

Speed [km/h]	Pant	Contact Force [N]								Contact loss			Steady Arm Uplift [m]
		F_{max}	F_{min}	ΔF	F_m	σ	σ / F_m	S_{max}	S_{Min}	$CL_{\#}$	CL_t [s]	$CL_{\%}$ [%]	
120	Single	298.5	-10.2	308.7	96.5	14.3	0.15	139.5	53.6	1	0.0	0.03	0.030
125	Single	285.5	-11.2	296.7	97.1	15.2	0.16	142.7	51.6	1	0.0	0.04	0.030
130	Single	280.9	-3.8	284.7	97.7	16.8	0.17	148.2	47.3	1	0.0	0.00	0.030
135	Single	277.0	0.0	277.0	98.3	18.7	0.19	154.5	42.1	0	0.0	0.00	0.030
140	Single	251.0	24.7	226.4	99.0	19.7	0.20	158.3	39.8	0	0.0	0.00	0.033
145	Single	212.1	50.8	161.3	99.6	19.7	0.20	158.6	40.7	0	0.0	0.00	0.035
150	Single	241.4	30.2	211.2	100.5	19.6	0.20	159.4	41.5	0	0.0	0.00	0.039
155	Single	188.4	57.8	130.6	101.0	19.8	0.20	160.5	41.6	0	0.0	0.00	0.043
160	Single	171.1	53.6	117.6	101.9	19.7	0.19	161.0	42.7	0	0.0	0.00	0.048
165	Single	207.1	41.5	165.6	102.5	19.1	0.19	159.8	45.2	0	0.0	0.00	0.059
170	Single	290.3	3.4	286.9	103.3	20.8	0.20	165.8	40.8	0	0.0	0.00	0.052
175	Single	345.8	-17.8	363.7	104.2	23.2	0.22	173.7	34.7	1	0.0	0.07	0.050

Table 4.2: LP10_Pant2_S0 results for simgle pantograph, running at various speeds

Speed [km/h]	Pant	Contact Force [N]								Contact loss			Steady Arm Uplift [m]
		F_{max}	F_{min}	ΔF	F_m	σ	σ / F_m	S_{max}	S_{Min}	$CL_{\#}$	CL_t [s]	$CL_{\%}$ [%]	
120	Single	283.8	-4.7	288.5	96.7	18.7	0.19	152.8	40.6	1	0.0	0.00	0.032
125	Single	247.3	31.5	215.8	97.1	18.7	0.19	153.3	41.0	0	0.0	0.00	0.034
130	Single	290.5	4.2	286.3	97.8	22.8	0.23	166.1	29.4	0	0.0	0.00	0.032
135	Single	246.5	42.4	204.1	98.4	23.5	0.24	168.8	28.1	0	0.0	0.00	0.033
140	Single	212.3	29.8	182.5	99.1	24.9	0.25	173.8	24.5	0	0.0	0.00	0.037
145	Single	181.8	47.4	134.4	99.6	24.0	0.24	171.7	27.6	0	0.0	0.00	0.040
150	Single	217.3	47.2	170.1	100.5	25.7	0.26	177.7	23.3	0	0.0	0.00	0.044
155	Single	178.2	42.3	135.9	101.1	26.2	0.26	179.8	22.4	0	0.0	0.00	0.045
160	Single	181.2	26.8	154.4	102.0	25.2	0.25	177.7	26.3	0	0.0	0.00	0.056
165	Single	248.4	-10.0	258.5	102.4	27.1	0.26	183.7	21.1	1	0.0	0.07	0.061
170	Single	305.6	16.0	289.6	103.1	28.8	0.28	189.7	16.6	0	0.0	0.00	0.055
175	Single	331.3	13.9	317.4	104.2	32.1	0.31	200.5	7.8	0	0.0	0.00	0.055

Looking at the LP12 catenary paired with the Pant1 pantograph the exploration velocity is found to be 260 km/h for a single pantograph train operation. Considering that the maximum operating velocity is 283 km/h, this catenary loses almost 23 km/h. The limiting parameter of this pantograph-catenary pair is the maximum contact force seen in Table 4.3 that is located in the section of the catenary with the overlap. Comparing the cases with the Pant1 pantograph and the Pant2 pantograph, it is possible to observe that the limiting parameter of this pantograph-catenary pair is also the maximum force

Table 4.2. However, the Pant2 operation has an exploration velocity, that is found to be 230 km/h, in Table 4.4, for a single pantograph train operation, this is a little bit lower than when using the Pant1 pantograph and it is close to 53 km/h lower than the maximum operating velocity. This pantograph catenary case limiting factor is the standard deviation. By comparing the dynamic analysis results for both pantographs, it is found that the standard deviation has higher values and lower the statistical minimum for the Pant2 pantograph simulations. This means that the limiting factor for the LP12_Pant2 case is the pantograph used, since it is known that this catenary paired with a different pantograph has a better contact force interaction

Table 4.3: LP12_Pant1_S0 results for simgle pantograph, running at various speeds

Speed [km/h]	Pant	Contact Force [N]								Contact loss			Steady Arm Uplift [m]
		F_{max}	F_{min}	ΔF	F_m	σ	σ /F_m	S_{max}	S_{Min}	$CL_{\#}$	CL_t [s]	$CL_{\%}$ [%]	
120	Single	134.0	67.0	67.0	96.6	10.0	0.10	126.7	66.5	0	0.0	0.00	0.019
130	Single	150.5	60.4	90.1	97.8	10.8	0.11	130.3	65.3	0	0.0	0.00	0.018
140	Single	143.7	63.8	80.0	99.1	12.0	0.12	135.2	62.9	0	0.0	0.00	0.017
150	Single	153.7	47.1	106.6	100.5	16.0	0.16	148.6	52.4	0	0.0	0.00	0.017
160	Single	160.9	55.3	105.5	102.0	17.0	0.17	152.9	51.1	0	0.0	0.00	0.019
170	Single	159.4	54.3	105.1	103.5	16.6	0.16	153.3	53.7	0	0.0	0.00	0.022
180	Single	158.5	61.9	96.7	105.1	17.3	0.16	157.0	53.2	0	0.0	0.00	0.027
190	Single	162.4	53.5	108.8	106.8	17.2	0.16	158.3	55.3	0	0.0	0.00	0.029
200	Single	186.8	62.3	124.5	108.7	17.3	0.16	160.7	56.7	0	0.0	0.00	0.031
210	Single	167.2	54.5	112.7	112.7	20.3	0.18	173.6	51.8	0	0.0	0.00	0.031
215	Single	173.2	58.6	114.6	114.8	23.0	0.20	183.9	45.8	0	0.0	0.00	0.035
220	Single	186.9	62.2	124.7	116.9	24.7	0.21	190.9	42.9	0	0.0	0.00	0.041
225	Single	197.5	59.7	137.8	119.0	25.6	0.22	195.9	42.2	0	0.0	0.00	0.047
230	Single	205.7	62.7	143.0	120.9	26.5	0.22	200.6	41.3	0	0.0	0.00	0.050
235	Single	212.7	62.1	150.6	123.4	27.1	0.22	204.8	42.1	0	0.0	0.00	0.060
240	Single	246.5	69.8	176.7	125.7	27.3	0.22	207.6	43.9	0	0.0	0.00	0.060
245	Single	300.2	11.5	288.7	127.9	28.3	0.22	212.7	43.1	0	0.0	0.00	0.063
250	Single	260.2	31.9	228.4	130.3	29.3	0.23	218.3	42.3	0	0.0	0.00	0.063
255	Single	319.9	11.3	308.6	132.9	31.5	0.24	227.3	38.5	0	0.0	0.00	0.068
260	Single	283.9	11.0	272.8	135.3	32.6	0.24	233.1	37.4	0	0.0	0.00	0.072
265	Single	380.1	-38.8	419.0	137.7	36.4	0.26	246.9	28.6	1	0.0	0.15	0.076

Table 4.4: LP12_Pant2_S0 results for simgle pantograph, running at various speeds

Speed [km/h]	Pant	Contact Force [N]								Contact loss			Steady Arm Uplift [m]
		F_{max}	F_{min}	ΔF	F_m	σ	σ /F_m	S_{max}	S_{Min}	$CL_{\#}$	CL_t [s]	$CL_{\%}$ [%]	
120	Single	156.0	11.3	144.7	96.7	11.5	0.12	131.2	62.2	0	0.0	0.0	0.018
130	Single	168.4	42.6	125.9	97.7	13.2	0.14	137.4	58.0	0	0.0	0.0	0.018
140	Single	167.6	54.5	113.1	99.1	15.5	0.16	145.5	52.8	0	0.0	0.0	0.018
150	Single	184.6	25.5	159.1	100.5	19.6	0.20	159.4	41.6	0	0.0	0.0	0.018
160	Single	166.6	47.3	119.3	102.0	20.0	0.20	162.1	41.9	0	0.0	0.0	0.020
170	Single	164.3	42.8	121.4	103.5	20.4	0.20	164.8	42.2	0	0.0	0.0	0.024
180	Single	176.0	54.7	121.4	105.2	21.2	0.20	168.8	41.5	0	0.0	0.0	0.029
190	Single	163.9	47.4	116.5	106.8	20.5	0.19	168.2	45.5	0	0.0	0.0	0.029
200	Single	193.1	48.5	144.6	108.6	21.9	0.20	174.4	42.8	0	0.0	0.0	0.031
210	Single	187.7	43.8	143.9	112.7	27.9	0.25	196.3	29.1	0	0.0	0.0	0.037
215	Single	204.2	45.8	158.4	114.7	30.6	0.27	206.6	22.9	0	0.0	0.0	0.042
220	Single	208.9	41.2	167.8	116.9	32.7	0.28	214.9	18.9	0	0.0	0.0	0.046
225	Single	210.9	35.6	175.2	118.8	34.3	0.29	221.6	15.9	0	0.0	0.0	0.051
230	Single	238.2	34.3	203.9	121.2	36.2	0.30	229.9	12.4	0	0.0	0.0	0.058
235	Single	247.1	35.4	211.7	123.4	37.4	0.30	235.5	11.2	0	0.0	0.0	0.059
240	Single	287.2	42.9	244.2	125.4	38.6	0.31	241.1	9.7	0	0.0	0.0	0.060
245	Single	294.3	36.1	258.2	127.5	38.9	0.31	244.2	10.8	0	0.0	0.0	0.061
250	Single	492.6	-50.1	542.7	129.1	54.1	0.42	291.3	-33.1	1	0.0	0.2	0.070
255	Single	974.4	-69.7	1044.2	131.6	87.6	0.67	394.4	-131.1	18	0.4	3.1	0.131
260	Single	613.1	-73.2	686.2	134.2	93.7	0.70	415.3	-146.9	34	0.5	4.7	0.102
265	Single	884.8	-83.1	967.9	136.0	98.6	0.73	431.8	-159.8	24	0.4	3.8	0.115

Comparing the two catenaries, it is possible to observe that the exploration of the LP12 is better, because of the higher explorations velocities that the train can operate, and because the difference of operating velocities and exploration velocities is higher for the LP10 catenary. The LP10 is the one that if a few changes are made to improve the contact interaction can have the greatest improvement.

4.2. Multiple Pantographs

When studying the operation condition of a railway vehicle on a catenary, the maximum operation speed will be when only one pantograph is running in the catenary. This occurs because the elastic propagation wave propagates forward and backward from the pantograph position. However, when the operation occurs under multiple pantograph conditions, in this case, two pantographs working simultaneously, both pantographs will generate a propagation wave. Which interferes with the contact characteristics of the catenary with the other pantograph. Normally the trailing pantograph suffers from the propagation wave generated by the leading pantograph, affecting the contact parameters of the trailing pantograph. However, for some pantograph separations, the leading pantograph is the one that tends to be affected by the propagation wave of the trailing pantograph.

Looking at the simulation results of the LP10_Pant2_S35, in Table 4.5, it is observed that the standard deviation, for 155 km/h surpasses the respective threshold. While for 150 km/h there is a maximum force exciding the 300 N

limit. So, the exploration velocity for a separation of 35 m is 145 km/h. This speed is 20 km/h inferior to the maximum in a single pantograph operation for the same pantograph catenary pairing. The limiting factor for the LP10_Pant2_S35 case is the maximum contact force on the leading pantograph.

The limiting factor for LP10_Pant2_S200, is the standard deviation for the trailing pantograph. Where, the exploration velocity is 135 km/h, this velocity is 15 km/h lower than the obtained from LP10_Pant2_S35 and 35 km/h inferior to when only one pantograph is operating. In Table 4.6 the standard deviation ratio has a value of 0.31, when the velocity considered is 135 km/h, which is above the standard threshold of 0.3. By observing the dynamic analysis results obtained from the LP10_Pant2_S200_V165 stands out, because at these speeds all the parameters represented in the figure respect the threshold limits. However, the trailing standard deviation is almost at the standard threshold of 0.3. This means that, if any system perturbation is found, the trailing standard deviation, for this speed, increases, leading to σ/F_m superior than standard threshold of 0.3. So, the exploration velocity of LP10_Pant2_S200 is 130 km/h and the limiting factor is the standard deviation of the trailing pantograph.

Table 4.5: LP10_Pant2_S35 results for multiple pantographs, running at various speeds

Speed [km/h]	Pant	Contact Force [N]								Contact loss			Steady Arm Uplift [m]
		F_{max}	F_{min}	ΔF	F_m	σ	σ /F_m	S_{max}	S_{Min}	$CL_{\#}$	CL_t [s]	$CL_{\%}$ [%]	
120	Leading	298.1	-8.9	307.0	96.6	19.0	0.20	153.4	39.7	1	0.0	0.05	0.041
	Trailing	251.0	4.8	246.2	96.6	18.5	0.19	152.2	41.0	0	0.0	0.00	
125	Leading	290.2	9.6	280.6	97.0	19.4	0.20	155.2	38.9	0	0.0	0.00	0.039
	Trailing	220.7	19.0	201.8	96.9	19.3	0.20	154.9	39.0	0	0.0	0.00	
130	Leading	293.0	-1.2	294.2	97.6	22.0	0.23	163.5	31.6	1	0.0	0.00	0.046
	Trailing	191.9	23.3	168.5	97.5	18.9	0.19	154.2	40.9	0	0.0	0.00	
135	Leading	295.2	6.4	288.9	98.2	23.4	0.24	168.5	27.9	0	0.0	0.00	0.051
	Trailing	177.4	40.8	136.6	98.1	18.0	0.18	152.0	44.1	0	0.0	0.00	
140	Leading	208.8	31.0	177.9	99.0	23.0	0.23	167.8	30.1	0	0.0	0.00	0.057
	Trailing	215.7	24.2	191.5	99.1	20.9	0.21	161.9	36.3	0	0.0	0.00	
145	Leading	175.6	32.5	143.1	99.2	22.9	0.23	167.9	30.5	0	0.0	0.00	0.057
	Trailing	294.8	20.3	274.5	99.4	24.8	0.25	173.6	25.1	0	0.0	0.00	
150	Leading	256.1	-10.8	266.8	100.3	25.5	0.25	176.7	24.0	1	0.0	0.07	0.058
	Trailing	345.5	22.3	323.2	100.3	28.4	0.28	185.7	15.0	0	0.0	0.00	
155	Leading	227.5	26.7	200.8	100.8	25.4	0.25	177.1	24.5	0	0.0	0.00	0.058
	Trailing	407.0	-22.5	429.5	100.6	33.7	0.34	201.8	-0.6	2	0.0	0.17	
160	Leading	213.4	6.9	206.5	101.9	27.8	0.27	185.2	18.5	0	0.0	0.00	0.062
	Trailing	427.6	-9.7	437.2	101.8	33.0	0.32	200.9	2.7	2	0.0	0.14	
165	Leading	199.3	25.7	173.6	102.7	29.9	0.29	192.4	13.1	0	0.0	0.00	0.059
	Trailing	398.6	2.9	395.6	102.7	36.8	0.36	213.1	-7.7	0	0.0	0.00	
170	Leading	208.3	14.3	194.0	103.1	32.2	0.31	199.7	6.4	0	0.0	0.00	0.069
	Trailing	344.2	-4.7	348.9	103.3	42.3	0.41	230.1	-23.5	1	0.0	0.07	
175	Leading	235.7	4.2	231.6	103.9	33.8	0.33	205.2	2.6	0	0.0	0.00	0.072
	Trailing	302.2	-2.5	304.7	104.0	43.1	0.41	233.4	-25.5	2	0.0	0.16	
180	Leading	323.3	0.6	322.7	105.0	36.5	0.35	214.4	-4.4	0	0.0	0.00	0.071
	Trailing	333.9	1.3	332.6	105.0	42.3	0.40	231.9	-21.9	0	0.0	0.00	

Table 4.6: LP10_Pant2_S200 results for multiple pantographs, running at various speeds

Speed [km/h]	Pant	Contact Force [N]								Contact loss			Steady Arm Uplift [m]
		F_{max}	F_{min}	ΔF	F_m	σ	σ /F_m	S_{max}	S_{Min}	$CL_{\#}$	CL_t [s]	$CL_{\%}$ [%]	
120	Leading	187.1	53.7	133.5	96.8	14.6	0.15	140.6	52.9	0	0.0	0.00	0.039
	Trailing	209.6	61.0	148.6	96.1	15.5	0.16	142.6	49.6	0	0.0	0.00	
125	Leading	248.8	29.3	219.5	97.2	18.9	0.19	154.0	40.5	0	0.0	0.00	0.038
	Trailing	273.0	-0.9	273.9	97.3	22.4	0.23	164.6	30.1	2	0.0	0.00	
130	Leading	291.2	2.4	288.8	97.7	22.8	0.23	166.0	29.3	0	0.0	0.00	0.033
	Trailing	198.9	42.9	156.0	97.9	23.2	0.24	167.5	28.3	0	0.0	0.00	
135	Leading	232.7	46.4	186.3	98.3	23.2	0.24	168.1	28.6	0	0.0	0.00	0.035
	Trailing	253.6	12.2	241.4	98.3	30.1	0.31	188.6	8.0	0	0.0	0.00	
140	Leading	203.5	26.5	177.0	98.9	24.8	0.25	173.3	24.4	0	0.0	0.00	0.048
	Trailing	356.4	-1.1	357.5	99.1	37.3	0.38	211.0	-12.8	1	0.0	0.03	
145	Leading	190.9	34.6	156.3	99.3	24.9	0.25	174.1	24.6	0	0.0	0.00	0.055
	Trailing	234.3	1.8	232.5	99.6	34.0	0.34	201.6	-2.4	0	0.0	0.00	
150	Leading	178.0	48.8	129.2	100.1	25.4	0.25	176.1	24.0	0	0.0	0.00	0.050
	Trailing	192.3	9.9	182.4	100.4	32.6	0.32	198.1	2.7	0	0.0	0.00	
155	Leading	182.5	31.4	151.1	101.0	26.3	0.26	179.9	22.1	0	0.0	0.00	0.051
	Trailing	298.2	2.0	296.2	101.0	34.3	0.34	203.9	-1.8	0	0.0	0.00	
160	Leading	168.8	53.5	115.2	101.8	20.2	0.20	162.6	41.1	0	0.0	0.00	0.051
	Trailing	344.3	-33.2	377.5	101.8	27.1	0.27	183.2	20.4	1	0.0	0.08	
165	Leading	184.8	12.9	171.9	102.0	27.3	0.27	183.9	20.1	0	0.0	0.00	0.070
	Trailing	282.9	-7.7	290.6	102.7	36.5	0.36	212.2	-6.8	1	0.0	0.07	
170	Leading	306.1	18.3	287.7	102.8	29.0	0.28	189.9	15.7	0	0.0	0.00	0.066
	Trailing	507.8	-30.8	538.6	103.4	39.4	0.38	221.5	-14.7	2	0.1	0.38	
175	Leading	306.2	21.5	284.7	103.9	29.9	0.29	193.7	14.0	0	0.0	0.00	0.066
	Trailing	295.3	-17.7	313.1	104.2	37.1	0.36	215.4	-7.0	3	0.0	0.22	

5. Conclusions

This work focusses on the interaction pantograph-catenary. Where it is visible that the LP12 catenary has a higher exploration velocity than LP10, when the same pantograph and pantograph separation is considered. As seen when comparing the simulations with the higher exploration in this case the LP12_Pant1_S0 can reach 260 km/h, without surpassing any parameters threshold. While this equivalent case simulation for the LP10 catenary, designated by LP12_Pant1_S0, has an exploration velocity of 170 km/h.

Comparing the pantographs used, the Pant1 pantograph has an advantage, since the exploring velocities for the cases where the Pant1 pantograph is operated are always higher than their equivalent cases considering the Pant2 pantograph. Besides this, the contact quality difference when using the Pant1 or the Pant2 pantograph is intensifies with the velocity. As seen when comparing the difference of velocities between LP10_Pant1_S0 to LP10_Pant2_S0 and LP12_Pant1_S0 to LP12_Pant2_S0. When the LP10 catenary is considered the difference of velocities between the cases is 5 km/h, however when the catenary is exchanged to one with higher exploration velocities LP12 the difference in velocities observed by the exchange of pantographs is 30 km/h. So the use of the Pant2 pantograph should not be used if operating the railway vehicle the Pant1 pantograph is an option. The Pant2 pantograph model has an unusual topology and nonlinearities.

Comparing the separations dynamic analysis results for LP10_Pant2 the exploration velocity is 130 km/h, where the critical separation is 200 m. This is because the exploration velocity for LP10_Pant2_35 is 145 km/h. Comparing this two cases it is possible to see that the limiting pantograph is differs for both of them being the leading pantograph for a 35 m separation and the trailing pantograph for a separation of 200 m. Here, it is possible to understand that the contact interaction of the system is dependent of the pantograph separation.

References

[1] Collina A, Bruni S. Numerical Simulation of Pantograph-Overhead Equipment Interaction. Vehicle System Dynamics [Internet]. 2002;38:261–291. Available from: http://www.tandfonline.com/doi/abs/10.1076/vesd.38.4.261.8286.

[2] Shing AWC, Wong PPL. Wear of pantograph collector strips. Journal of Rail and Mass Transit [Internet]. 2008;222:169–176. Available from: http://journals.sagepub.com/doi/10.1243/09544097JRRT156.

[3] Bucca G, Collina A. A Procedure for the Wear Prediction of Collector Strip and Contact Wire in Pantograph-Catenary System. Wear. 2009;266:46–59.

[4] Poetsch G, Evans J, Maisinger R, et al. Pantograph/Catenary Interaction and Control. Vehicle System Dynamics. 1997;28:159–195.

[5] Oura Y, Mochinaga Y, Nagasawa H. Railway Electric Power Feeding Systems. Japan Railway & Transport Review. 1998;16:48–58.

[6] Ambrósio J, Pombo J, Pereira M, et al. A computational procedure for the dynamic analysis of the catenary-pantograph interaction in high-speed trains. Journal of Theoretical and Applied Mechanics. 2012;50.

[7] Ambrósio J, Pombo J, Antunes P, et al. PantoCat statement of method. Vehicle System Dynamics. 2015;53:314–328.

[8] Antunes P, Ambrósio J, Pombo J. Catenary finite element model initialization using optimization. Civil-Comp Proceedings. 2016;110.

[9] EN 50119:2020 Railway applications - Fixed installations - Electric traction overhead contact lines. CENLEC; 2020.

[10] Bathe K-J. Finite element procedures. Englewood Cliffs, N.J.: Prentice Hall; 1996.

[11] Przemieniecki JS. Theory of Matrix Structural Analysis. New York: McGraw-Hill; 1968.

[12] Newmark N. A Method of Computation for Structural Dynamics. ASCE Journal of the Engineering Mechanics Division. 1959;85:67–94.

[13] Vyasarayani CP, Uchida T, Carvalho A, et al. Parameter identification in dynamic systems using the homotopy optimization approach. Multibody System Dynamics. 2011;26:411–424.

[14] Ambrósio J, Pombo J, Pereira M, et al. Recent Developments in Pantograph-Catenary Interaction Modelling and Analysis. International Journal of Railway Technology [Internet]. 2012;1:249–278. Available from: http://www.ctresources.info/ijrt/paper.html?id=12.